

# Distinct rhythm generators for inspiration and expiration in the juvenile rat

Wiktor A. Janczewski and Jack L. Feldman

Department of Neurobiology, David Geffen School of Medicine at University of California, Los Angeles, Box 951763, Los Angeles, CA 90095-1763, USA

**Inspiration and active expiration are commonly viewed as antagonistic phases of a unitary oscillator that generates respiratory rhythm. This view conflicts with observations we report here in juvenile rats, where by administration of fentanyl, a selective  $\mu$ -opiate agonist, and induction of lung reflexes, we separately manipulated the frequency of inspirations and expirations. Moreover, completely transecting the brainstem at the caudal end of the facial nucleus abolished active expirations, while rhythmic inspirations continued. We hypothesize that inspiration and expiration are generated by coupled, anatomically separate rhythm generators, one generating active expiration located close to the facial nucleus in the region of the retrotrapezoid nucleus/parafacial respiratory group, the other generating inspiration located more caudally in the preBöttinger Complex.**

(Received 19 September 2005; accepted after revision 10 November 2005; first published online 17 November 2005)

**Corresponding author** W. A. Janczewski: Department of Neurobiology, David Geffen School of Medicine, Box 951763, 10833 LeConte Avenue, Los Angeles, CA 90095-1763, USA. Email: victoraj@mednet.ucla.edu

Rhythmic movements in mammals are cyclical sequences of precise patterns of muscle contraction and relaxation typically divided in phases – locomotion: swing/stance; mastication: open/close; and breathing: inspiration/expiration. There are two distinct views as to the general underlying neuronal organization. In one view, a single-rhythm generator paces the whole cycle, with interneuronal circuits dividing the cycle into appropriately timed bursts in specific muscles. This is the longstanding view of how respiratory rhythm is generated: a single rhythm generator produces two (inspiration, expiration) or three (inspiration, postinspiration, expiration) phases with distinct muscle activation patterns in each phase. In single-rhythm generator models for respiratory rhythm, both the ‘two-phase’ (Feldman & Cowan, 1975) and ‘three-phase’ (Richter, 1982; Richter *et al.* 1992; Rybak *et al.* 1997) variants require reciprocal synaptic inhibition between groups of sequentially active interneurons to produce phasing.

An alternative view of rhythmic movement is that independent coupled rhythm generators spawn distinct phases. For example, in one model for the generation of locomotion, mechanically distinct portions of the cycle have their own rhythm generators, which then coordinate amongst themselves (Kudo & Yamada, 1987; Grillner, 1991; Grillner & Wallen, 2002).

We recently proposed that respiratory rhythm is generated by two coupled anatomically distinct rhythm generators (Feldman *et al.* 2003; Mellen *et al.* 2003), one in the preBöttinger Complex (preBötC; Smith *et al.* 1991),

and the other in the retrotrapezoid nucleus/parafacial respiratory group (RTN/pFRG; Feldman *et al.* 2003; Onimaru & Homma, 2003). This hypothesis emerged from analysis of cellular mechanisms leading to a quantal pattern of breathing induced by administration of opioids (Feldman *et al.* 2003; Mellen *et al.* 2003). In brief, preinspiratory (pre-I) neurones in the RTN/pFRG are unaffected by opioids, continuing to generate rhythmic activity without any change in burst frequency (Takeda *et al.* 2001). In contrast, many preBötC neurones are inhibited by opioids; in *en bloc* preparations *in vitro* they burst rhythmically and concurrently with inspiratory nerve motor output, but show only subthreshold activity during cycles of pre-I activity where there is no inspiratory motor output (Mellen *et al.* 2003). On the basis of this cellular data, we proposed a two-rhythm generator hypothesis for the generation of respiratory rhythm (Feldman *et al.* 2003; Mellen *et al.* 2003). The functional role of these rhythm generators in terms of ventilation and muscle activity remains to be determined. Here, we refine this hypothesis to propose that one rhythm generator produces inspirations, and the other produces active expirations.

To test the two-rhythm generator hypothesis for breathing, we aimed to uncouple inspiratory from expiratory motor activity to an extent that would be improbable if a unitary multiphase rhythm generator drove the breathing cycle. We used two experimental perturbations that differentially affect inspiratory and expiratory activity: (i) opioid administration, which

depresses inspiratory (Gray *et al.* 1999; Takeda *et al.* 2001; Mellen *et al.* 2003) more than expiratory (Howard & Sears, 1991; Janczewski *et al.* 2002; Drummond, 2003) activity; (ii) positive or negative airway pressure to manipulate lung volume in order to elicit pulmonary afferent, commonly referred to as the Breuer-Hering reflexes: the Breuer-Hering deflation reflex facilitates inspiratory activity and depresses expiratory activity, while the Breuer-Hering inflation reflex has the opposite effect (Feldman, 1986).

Preliminary results were presented in an abstract form (Janczewski & Feldman, 2002, 2003).

## Methods

### Animals and procedures

Experiments were performed on Sprague-Dawley juvenile rats (postnatal day 7–13) of both sexes, and weight in the range 16–32 g. At this stage, their central nervous system development corresponds to a period from birth to 3 months of age in human (Ballanyi, 2004). The UCLA Animal Research Committee approved all experimental protocols.

Rats ( $n = 29$ ) were anaesthetized with ketamine ( $50 \text{ mg kg}^{-1}$ , Ketaject; Phoenix Pharmaceutical, Inc., St Joseph, MO, USA) and, except for rats studied for baseline data ( $n = 6$ ), supplemented with fentanyl citrate ( $20 \text{ } \mu\text{g kg}^{-1}$ ; Abbott Laboratories, North Chicago, IL, USA) administered subcutaneously (s.c.; Katz *et al.* 1993; Wixson & Smiler, 1997; Sakamoto *et al.* 2001). In order to eliminate spontaneous non-respiratory motor activity and respiratory drives from the forebrain (Ballanyi, 2004), the occipital bone was partly removed and the midbrain was transected in all rats. The level of anaesthesia was assessed by suppression of the withdrawal reflex, and by the absence of changes in heart rate and breathing rate in response to noxious stimuli. A polyethylene cannula (1.2 mm o.d.; A-M Systems, Sequim, WA, USA) was inserted via the mouth into the trachea, and rats were mechanically ventilated (Model 683, Harvard Apparatus, Holliston, MA, USA). EMG wire electrodes (Cooner Wire Co., Chatsworth, CA, USA) were implanted into the abdominal oblique and genioglossus muscles.

### Experimental protocol

Each preparation was ventilated and allowed to stabilize for 40–60 min after midbrain, and any subsequent additional, transection. Then, the tracheal cannula was connected to a device to measure airflow (MLT1L; ADInstruments, Colorado Springs, CO, USA). Except where noted, rats breathed a hyperoxic mixture (1:3, air:O<sub>2</sub>) throughout the experiment. After control recordings, fentanyl ( $10 \text{ } \mu\text{g kg}^{-1}$  s.c.) was injected once or several times until the onset

of quantal breathing (Fig. 1). A sufficient total dose was  $40 \text{ } \mu\text{g kg}^{-1}$  in every rat. We refer to cycles with abdominal muscle electromyographic (EMG<sub>ABD</sub>) bursts but no inspiratory motor activity as ‘E-only cycles’. We refer to cycles that maintained the normal sequence of expiratory and inspiratory motor activity as ‘I-E cycles’. In order to determine the mean period of the E-only cycles ( $\overline{P_{E\text{-only}}}$ ) and the mean period of the I-E cycles ( $\overline{P_{I-E}}$ ) for each rat, we analysed a continuous record containing 100 E-only cycles and >100 I-E cycles (see Fig. 2A). Over time, after injection of fentanyl (20–40 min), the rate of occurrence of E-only cycles decreased. In order to increase the number of E-only cycles, we injected one or more additional doses of fentanyl ( $10 \text{ } \mu\text{g kg}^{-1}$  s.c.).

To manipulate lung volume, we changed pulmonary pressure by connecting the tracheal cannula to a pressure source gated by an electronic valve. We applied continuous positive airway pressure (CPAP; 3–5 cmH<sub>2</sub>O or  $\sim 9 \text{ cmH}_2\text{O}$ ) or negative pressure (–1 to –4 cmH<sub>2</sub>O) during a period of several cycles or positive pressure pulses <1 s in duration (brief inflations).

Five rats with intact vagi received naloxone ( $0.03 \text{ mg kg}^{-1}$  s.c.). This dose was 20 times lower than that necessary to reverse fentanyl-induced respiratory depression (unpublished observations).

### Transection experiments

Transections were performed with a knife made of a 1.5 mm wide piece of razor blade fixed in a micromanipulator (Janczewski & Karczewski, 1984, 1990). As mentioned above, at the beginning of an experiment the midbrain was transected at the midcollicular level. In 15 rats from this group (seven with vagi intact, eight with vagotomy) that did not receive naloxone, additional transections at various levels of the brainstem were performed. Ten minutes before each transection, rats were ventilated with 1–2 vol% isoflurane in O<sub>2</sub> (IsoFlo; Abbott Laboratories, North Chicago, IL, USA). Isoflurane was terminated 2 min after each transection. (Isoflurane was used to induce controlled hypotension (Madsen *et al.* 1987; Ringaert & Mutch, 1988) and for its neuroprotective properties (Homi *et al.* 2003)). The initial brainstem transection was placed at the rostral end of the facial nucleus. This transection eliminated the descending influence of the pons (and all suprapontine structures) on breathing. Additional transections (0.2 mm apart) were made in five rats at progressively more caudal levels to ultimately eliminate the influence of RTN/pFRG (Feldman *et al.* 2003; Onimaru & Homma, 2003) on breathing. Following some transections, there was a transient loss of respiratory activity, lasting up to 10 min, at which point both inspiratory and expiratory motor, i.e. EMG<sub>ABD</sub> bursts, activity returned. Finally, a transection

at the level 'caudal-t' in Fig. 7C eliminated EMG<sub>ABD</sub>, but not inspiratory activity. At this point the preparation was allowed to stabilize for ~1 h before recordings commenced ( $n = 5$ ). Recordings were taken for 30 min. At the end of this period we occluded the tracheal tube for 1 min to test whether anoxia could restore EMG<sub>ABD</sub> bursts. We assumed that EMG<sub>ABD</sub> bursts were effectively eliminated when they were absent for 1.5 h and did not reappear in response to anoxia. During transections and during recovery, rats were mechanically ventilated with 100% O<sub>2</sub> to maintain haemoglobin saturation ( $S_{aO_2}$ ; >90%, as measured with a pulse oximeter, Model 8600 V, Nonin Medical, Inc., Plymouth, MN, USA).

Rats were killed with an overdose of pentobarbitone (100 mg kg<sup>-1</sup> i.p.) and the brainstems removed. To determine the transection plane, brainstems were kept for 3 days in 4% paraformaldehyde, overnight in a 30% sucrose solution, sectioned (40  $\mu$ m) with a cryostat, stained with neutral red, and examined with a research microscope.

### Data analysis

To calibrate the flow and/or volume, 0.1, 0.2 and 0.3 ml of air was delivered from a syringe connected to the flow head before taking measurements, and the ratio between the integral of the flow and delivered volume was determined. EMG<sub>ABD</sub> and genioglossus muscle electromyographic (EMG<sub>GG</sub>) signals were amplified (Grass Model P511K; Grass Instrument Co., West Warwick, RI, USA). The absolute values of the EMG<sub>ABD</sub> and EMG<sub>GG</sub> signals were digitally integrated with a time constant ( $\tau$ ) of 0.1 s. The amplitude of the integrated signal was used as a measure of EMG activity (see Fig. 2B). The flow signal was high-pass filtered to eliminate DC shifts and slow drifts, with the cut-off frequency set for each recording at the lowest effective frequency (range 0–0.4 Hz). After filtering, the flow signal was digitally integrated to obtain  $V_T$ . Intratracheal pressure was continuously measured with a pressure transducer.

Signals were sampled at 1 kHz (Powerlab 16SP; ADInstruments) and analysed using Chart 5 (ADInstruments) and Igor Pro (WaveMetrics, Lake Oswego, OR, USA) software. Custom Igor Pro algorithms recognized and distinguished between E-only and I-E cycles. Cycle periods were calculated from the beginning of each EMG<sub>ABD</sub> bursts to the next one. Reported group mean values are group means for all rats. Mean values for every rat were calculated from 100 consecutive respiratory cycles. Recordings presented in figures are representative for all rats.

Expiratory frequency ( $f_E$ ) was the number of EMG<sub>ABD</sub> bursts per minute. Inspiratory frequency was the number of inspirations per minute, as determined from the

flow signal ( $f_I$ ). Statistical analysis was performed by Student's  $t$  test and paired  $t$  test. A  $P$  value of 0.05 or less was considered significant. All results are expressed as means  $\pm$  standard deviation.

## Results

### Breathing pattern in anaesthetized midbrain-decerebrate juvenile rats

Studies were performed in midbrain-transected (to eliminate spontaneous nonrespiratory motor activity and respiratory drives from the forebrain) juvenile rats anaesthetized with ketamine, with intact or cut vagi. Prior to administration of fentanyl, rats with intact vagi breathed with the normal repeating sequence of inspiration and expiration (I-E cycles;  $n = 6$ ). Inspiration was defined by inspiratory flow and the absence of EMG<sub>ABD</sub> bursts; expiration was defined by EMG<sub>ABD</sub> (present in all rats), which was tonic ( $n = 3$ ) or decrementing ( $n = 3$ ) in the period between inspirations. The group mean respiratory period ( $\overline{P_{I-E}}$ ) was  $0.6 \pm 0.1$  s and the (group mean) frequency was  $106.7 \pm 20.9$  breaths min<sup>-1</sup> (range 87–145). Vagotomy prolonged the respiratory period ( $\overline{P_{I-E}}$ ,  $2.7 \pm 0.4$  s; frequency,  $22.9 \pm 3.0$  breaths min<sup>-1</sup>;  $P < 0.01$ ,  $n = 6$ ), with expiration having two components (Fig. 1A). The first part of expiration was characterized by decrementing or tonic EMG<sub>ABD</sub>; the second part, i.e. active expiration, was defined by a phasic burst of EMG<sub>ABD</sub> (Bianchi *et al.* 1995). Peak EMG<sub>ABD</sub> amplitude increased to  $262.2 \pm 44.3\%$  of the peak in vagus-intact rats ( $P < 0.01$ ).

### Characteristics of quantal breathing in vagotomized rats given fentanyl

Fentanyl (10–20  $\mu$ g kg<sup>-1</sup> s.c.), a synthetic, selective  $\mu$ -opiate agonist, caused quantal breathing (Mellen *et al.* 2003), i.e. the occasional absence of inspiration manifested as a sequence of two or more consecutive expirations (Figs 1B, and 2A and B). At a higher dose of fentanyl (20–40  $\mu$ g kg<sup>-1</sup> s.c.), inspiration, when it occurred, was coincident with a pause during the EMG<sub>ABD</sub> burst ( $n = 7$  of 9; Figs 1C and 2B: cycles 1, 3, 6, 8 and 9, Fig. 2C), and there was an increase in the number of cycles with EMG<sub>ABD</sub> bursts that were not paired with an inspiration (E-only cycles), e.g. Figs 1C and 2B: cycles 2, 4, 5 and 7. EMG<sub>GG</sub> had two components, a burst during inspiration (I-EMG<sub>GG</sub>) in all rats ( $n = 8$ ), and a burst during active expiration (E-EMG<sub>GG</sub>; Figs 1A and 2C) in some rats ( $n = 5$  out of 8). During E-only cycles, E-EMG<sub>GG</sub>, but not I-EMG<sub>GG</sub>, was present (Fig. 2B and D).

Differences between I-E and E-only cycles were the same in every rat: (i) I-E cycles were longer than E-only cycles ( $\overline{P_{I-E}}$ ,  $4.4 \pm 1.3$  s;  $\overline{P_{E-only}}$ ,  $3.7 \pm 1.0$  s;  $P < 0.01$ ,  $n = 8$ );

(ii) the duration of  $EMG_{GG}$  activity during I-E cycles was longer than during E-only cycles (by  $32.4 \pm 22.7\%$ ;  $P < 0.05$ ,  $n = 6$ ; Fig. 2D, top); (iii) during I-E cycles, the  $EMG_{ABD}$  burst was split in two, with a total duration that was longer than that during E-only cycles (by  $42.9 \pm 26.2\%$ ;  $P < 0.01$ ,  $n = 8$ ; Fig. 2D, bottom).

During E-only cycles, expiratory flow produced by each  $EMG_{ABD}$  burst reduced lung volume below resting levels, e.g. Figure 2B; also Figs 1, 3, 5 and 6. Consequently, the lung and rib cage passively expanded, resulting in inspiratory airflow back to resting lung volume. This pattern of breathing, with passive inspiration following active expiration, is common in reptiles (Brainerd, 1999).

### Transections of the pons between the V and VII nuclei increased $f_E$

As opiates can affect the pons to modulate breathing pattern *in vitro* (Tanabe *et al.* 2005), we tested whether it was essential for quantal breathing *in vivo* by removing its influence on breathing with a complete transection placed rostral to the VII nucleus and caudal to the V nucleus ('rostral-t' in Fig. 7C;  $n = 15$ : seven with vagi intact, eight with vagotomy). This transection increased  $f_E$ , but the quantal breathing pattern remained, in both vagus intact (Figs 3 and 5) and vagotomized rats given fentanyl. In all rats, respiratory period was considerably shorter following this pontine transection. In vagotomized rats,  $\overline{P}_{I-E}$  dropped from  $4.4 \pm 1.3$  s in midbrain-transected rats to  $2.9 \pm 0.5$  s in pontine-transected rats ( $P < 0.05$ ,  $n = 8$ ) and  $\overline{P}_{E-only}$  dropped from  $3.7 \pm 1.0$  to  $2.5 \pm 0.5$  s ( $P < 0.05$ ,  $n = 8$ );  $f_E$

was in the range of 18–32 bursts  $\text{min}^{-1}$ . In vagus intact rats,  $\overline{P}_{I-E}$  dropped from  $3.6 \pm 0.7$  s in midbrain-transected rats to  $1.7 \pm 0.6$  s in pontine-transected rats ( $P < 0.01$ ,  $n = 7$ ) and  $\overline{P}_{E-only}$  dropped from  $3.6 \pm 0.6$  to  $1.7 \pm 0.6$  s ( $P < 0.01$ ,  $n = 7$ );  $f_E$  was in the range of 21–61 bursts  $\text{min}^{-1}$ . Regardless of whether the pons was detached (Fig. 3) or intact, split  $EMG_{ABD}$  bursts were rare in vagus-intact rats. This single  $EMG_{ABD}$  burst pattern was in marked contrast to a two-burst  $EMG_{ABD}$  pattern of vagotomized rats given fentanyl.

### Effects of lung volume manipulations on $f_I$ and $f_E$ in vagus-intact rats

In rats with intact vagi we used the Breuer-Hering reflexes to separately control  $f_I$  and  $f_E$ , because these vagal reflexes differentially affect inspiration and expiration (Feldman, 1986). Increased lung volume can prematurely terminate inspiratory and facilitate expiratory activity, acting to prevent lung overinflation (Breuer-Hering inflation reflex), whereas reduced lung volume facilitates inspiratory and inhibits expiratory activity, acting to restore normal lung volume (Breuer-Hering deflation reflex) (Porter, 1970; Feldman, 1986).

**Lung inflation.** Sustained increases in lung volume were produced by CPAP. CPAP of 3–5 cm  $\text{H}_2\text{O}$  eliminated all inspirations ( $f_I = 0$ ), but rhythmic expirations continued in every rat; there were increases in both  $EMG_{ABD}$  burst amplitude (by  $29.0\% \pm 14.5\%$ ,  $P < 0.01$ ) and duration (by  $26.6\% \pm 11.3\%$ ,  $P < 0.01$ ,  $n = 6$ ; Fig. 3). At higher CPAP

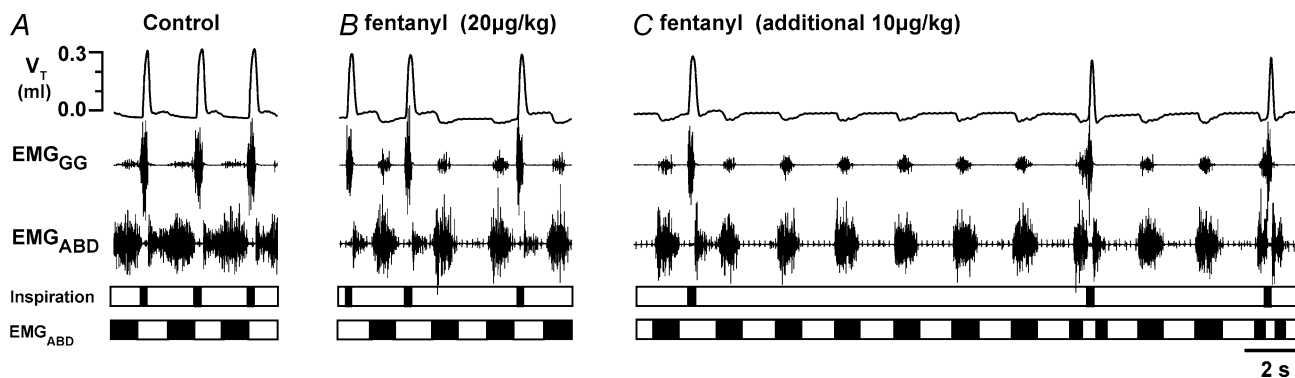


**Figure 1. Transition from control to quantal pattern of breathing in an 11-day-old vagotomized rat after fentanyl**

Top three traces, recordings of tidal volume ( $V_T$ ), genioglossus muscle electromyographic ( $EMG_{GG}$ ) and abdominal muscle electromyographic ( $EMG_{ABD}$ ) activity. Bottom, timing bars indicating occurrence of inspiratory airflow (inspiration) and expiratory motor activity ( $EMG_{ABD}$ ). *A*, control recording had all normal (I-E) cycles (i.e. cycles with inspiration and expiration). *B*, onset of quantal breathing (as an occasional sequence of inspiration–expiration–expiration, i.e. E-only cycle (cycle without inspiration), is observed at 9 min after an initial dose of fentanyl ( $20 \mu\text{g kg}^{-1}$  s.c.). *C*, at 4 min after a supplemental dose of fentanyl ( $10 \mu\text{g kg}^{-1}$ ), there are more E-only cycles. Note split  $EMG_{ABD}$  bursts in I-E cycles, and single  $EMG_{ABD}$  burst in E-only cycles.

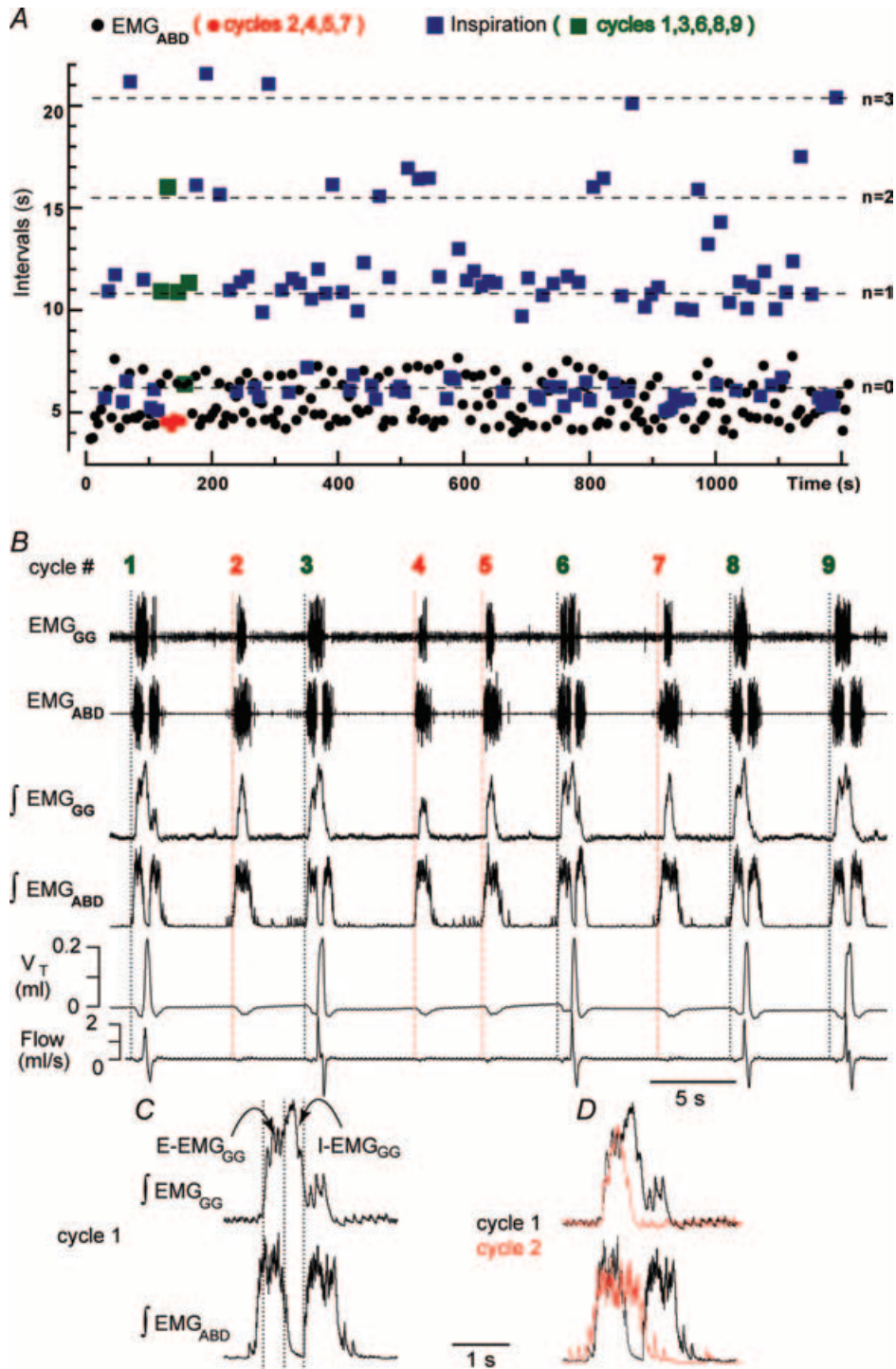


**Figure 2. Quantal pattern of breathing in an 8-day-old vagotomized rat given fentanyl**

*A*, intervals between successive EMG<sub>ABD</sub> bursts (circles) and inspirations (squares) for 220 consecutive respiratory cycles: 120 I-E cycles (mean duration of I-E cycles ( $\overline{P_{I-E}}$ ) = 6.2 s) and 100 E-only cycles (mean duration of E-only cycles ( $\overline{P_{E-only}}$ ) = 4.6 s). *B*, recording of epoch shown in *A* (~150 s, 190 s); green squares represent normal, i.e. I-E cycles (1, 3, 6, 8, 9), and red circles represent E-only cycles (2, 4, 5, 7). Traces from top to bottom: cycle number, EMG<sub>GG</sub>, EMG<sub>ABD</sub>, their integrals (∫EMG<sub>GG</sub> and ∫EMG<sub>ABD</sub>), V<sub>T</sub> and respiratory flow. Vertical dotted lines mark the onset of each EMG<sub>ABD</sub> burst. E-only cycles differed from I-E cycles; see *C*, *D* and text. *C*, ∫EMG<sub>GG</sub> and ∫EMG<sub>ABD</sub> on an expanded time scale to show pattern of bursting in an I-E cycle (cycle 1); note that ∫EMG<sub>GG</sub> has two distinct components (I-EMG<sub>GG</sub> and E-EMG<sub>GG</sub>) and can have no delay between them or be separate, e.g. Fig. 3, paired vertical lines. EMG<sub>ABD</sub> activity has a two-burst structure. *D*, comparison of an I-E cycle (cycle 1) and an E-only cycle (cycle 2, red).

( $\sim 9$  cmH<sub>2</sub>O), EMG<sub>ABD</sub> activity became tonic in all rats (Supplemental Fig. 1A and Video 1).

An alternative method to elicit the inflation reflex is to apply one or a series of brief lung inflations; this resulted in inhibition of inspiratory activity and excitation of expiratory activity (Fig. 4A). In control, i.e. without fentanyl, juvenile rats, EMG<sub>ABD</sub> activity ceased for 40–140 ms at the beginning of each inflation (Fig. 4A), indicating transient inhibition or resetting of expiratory activity. After administration of fentanyl, brief rhythmic lung inflations initiated during an EMG<sub>ABD</sub> burst decreased its duration, and when triggered at the onset of successive bursts they increased  $f_E$  (Fig. 4C). The maximal values of  $f_E$  were obtained when EMG<sub>ABD</sub> bursts were terminated shortly (0.1–0.3 s) after burst onset, in which case  $f_E$  increased from  $17.9 \pm 3.4$  cycles min<sup>-1</sup> to  $29.3 \pm 5.0$  cycles min<sup>-1</sup> ( $P < 0.05$ ,  $n = 6$ ). Brief inflations between EMG<sub>ABD</sub> bursts either prolonged or did not change the interburst interval. Brief deflations during the EMG<sub>ABD</sub> bursts triggered inspiration and terminated EMG<sub>ABD</sub> bursts (Fig. 4D and D-1).

**Lung deflation.** Sustained reduction of lung volume by lung deflation increased  $f_I$  but had no effect or decreased  $f_I$  ( $n = 6$ ); consequently, the  $f_I/f_E$  ratio increased. In Fig. 5 at atmospheric pressure (applied tracheal pressure, 0 cmH<sub>2</sub>O),  $f_I/f_E = 0.7$  (36/60 cycles min<sup>-1</sup>). Lung deflation ( $-1.5$  cmH<sub>2</sub>O) recruited additional inspirations so that  $f_I/f_E = 1$ , the value for this ratio in control conditions. Increased negative pressure ( $-3$  cmH<sub>2</sub>O) recruited even more inspirations, so that  $f_I/f_E$  was 2.5. Ectopic inspirations recruited by lung deflation (marked by triangles in Fig. 5) could be differentiated from those that were part of an I-E cycle (marked by arrows in Fig. 5): (i) they were not preceded by a sustained EMG<sub>ABD</sub> burst; and (ii) they were smaller than inspirations preceded by a sustained EMG<sub>ABD</sub> burst.

Thus, with pressure of  $-3$  cmH<sub>2</sub>O, two distinct rhythms of inspiratory activity were seen. One was locked to the rhythm of EMG<sub>ABD</sub> bursts, and the other had higher frequency and smaller amplitude (Fig. 5). (Supplemental Fig. 1B and Video 2 show the response to lung deflation).

### Effects of naloxone on $f_I$ and $f_E$ in vagus-intact rats

A selective increase in  $f_I$  leading to  $f_I/f_E > 1$ , similar to that induced by lung deflation, could also be induced by administration of a low dose of the  $\mu$ -opiate-antagonist naloxone ( $0.03$  mg kg<sup>-1</sup> s.c.) in rats given fentanyl regardless whether the vagi were cut ( $n = 4$ ) or intact ( $n = 5$ , Fig. 6). Inspirations preceded by EMG<sub>ABD</sub> bursts were larger (by  $26.4\% \pm 9.8$ ;  $P < 0.01$ ,  $n = 5$ ) than ectopic inspirations (Fig. 6). Rats that received naloxone were not used for any further protocol.

### EMG<sub>ABD</sub> bursts were eliminated by a specific brainstem transection in vagotomized rats

Five rats with the pontine transections described above spontaneously recovered from the fentanyl-induced quantal pattern of breathing, and were used to investigate whether neural structures required to generate inspiration are separate from those required to generate active expiration. Rats were vagotomized and mechanically ventilated with a hyperoxic gas mixture (100% O<sub>2</sub>) to assure stable blood gas levels and avoid hypoxia. The first transection in this series in each rat was made just rostral to the VII nucleus (Fig. 7C, marked as 'rostral-t'). Additional transections were made at progressively more caudal levels of the VII nucleus until rhythmic EMG<sub>ABD</sub> bursts were eliminated. After the final transection (Fig. 7C, marked as 'caudal-t'), inspirations and low-amplitude tonic EMG<sub>ABD</sub> activity (inhibited during inspiration)

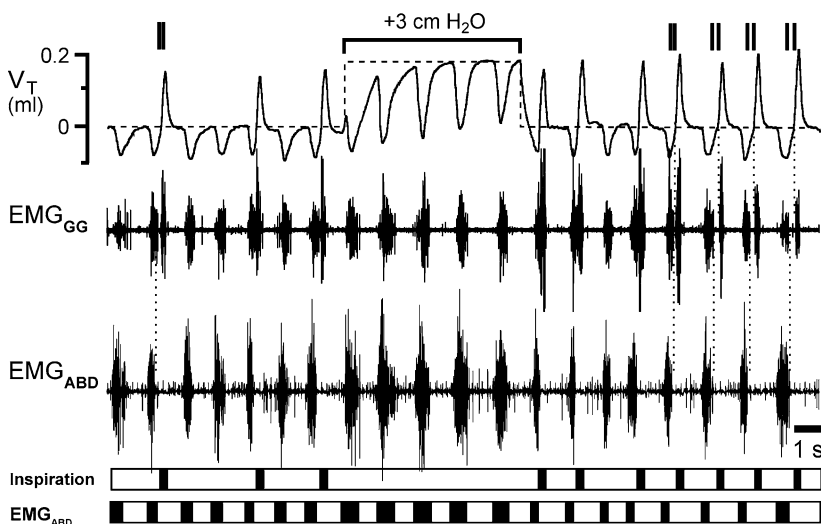


**Figure 3. Response to continuous positive airway pressure (CPAP) in an 11-day-old rat with intact vagi and transected pons given fentanyl**

Top traces,  $V_T$  (continuous line) with superimposed resting lung volume (dashed line), EMG<sub>GG</sub> and EMG<sub>ABD</sub>. Paired vertical lines above the  $V_T$  trace indicate I-E cycles where termination of an I-EMG<sub>GG</sub> burst and onset of subsequent E-EMG<sub>GG</sub> burst were separate; this is consistent with distinct sources of these bursts. Bottom, timing bars (see Fig. 1). Initially, inspiratory frequency/expiratory frequency ( $f_I/f_E$ ) = 0.7, i.e. on average 3 of 10 cycles were E-only. With CPAP = 3 cmH<sub>2</sub>O,  $f_I/f_E = 0$ , as I-E cycles were completely suppressed. Note that during CPAP the amplitude and duration of the expiratory efforts increased, and  $V_T$  generated by 'passive' inflations matched that of active inspirations.

were observed (Fig. 7B).  $f_I$  was  $21.1 \pm 2.7$  cycles  $\text{min}^{-1}$  after the transection marked 'rostral-t' and increased to  $25.4 \pm 2.0$  cycles  $\text{min}^{-1}$  ( $P < 0.05$ ) after the last transection marked 'caudal-t'.  $\text{EMG}_{\text{ABD}}$  was monitored for 1.5 h after the last transection; burst activity did not return in any rat. Occluding the airways for 1 min to induce anoxia failed to restore  $\text{EMG}_{\text{ABD}}$  bursting.

Transections were complete as determined by examination *in situ* and in the subsequent histological examination. *In situ* examination revealed that the medulla caudal to the 'caudal-t' transection was completely detached from the more rostral medulla. For histology, the tissue was cut parallel to the plane of the 'caudal-t' transection. Histological examination revealed: (i) that the most caudal transections, which irreversibly

eliminated  $\text{EMG}_{\text{ABD}}$  bursts, were placed at the caudal end of the facial nucleus (marked 'caudal-t' in Fig. 7;  $n = 5$ ); and (ii) no apparent damage to the medulla just caudal to the last transection, especially in the region containing the BötC.

## Discussion

By administering a selective  $\mu$ -opiate agonist, eliciting pulmonary reflexes, and transecting the brainstem, we manipulated the respiratory pattern in juvenile rodents in a way that suggests that anatomically separate, functionally distinct rhythm generators are coupled to spawn inspiration and active expiration in juvenile rats. Normally, bursts of inspiratory and expiratory motor

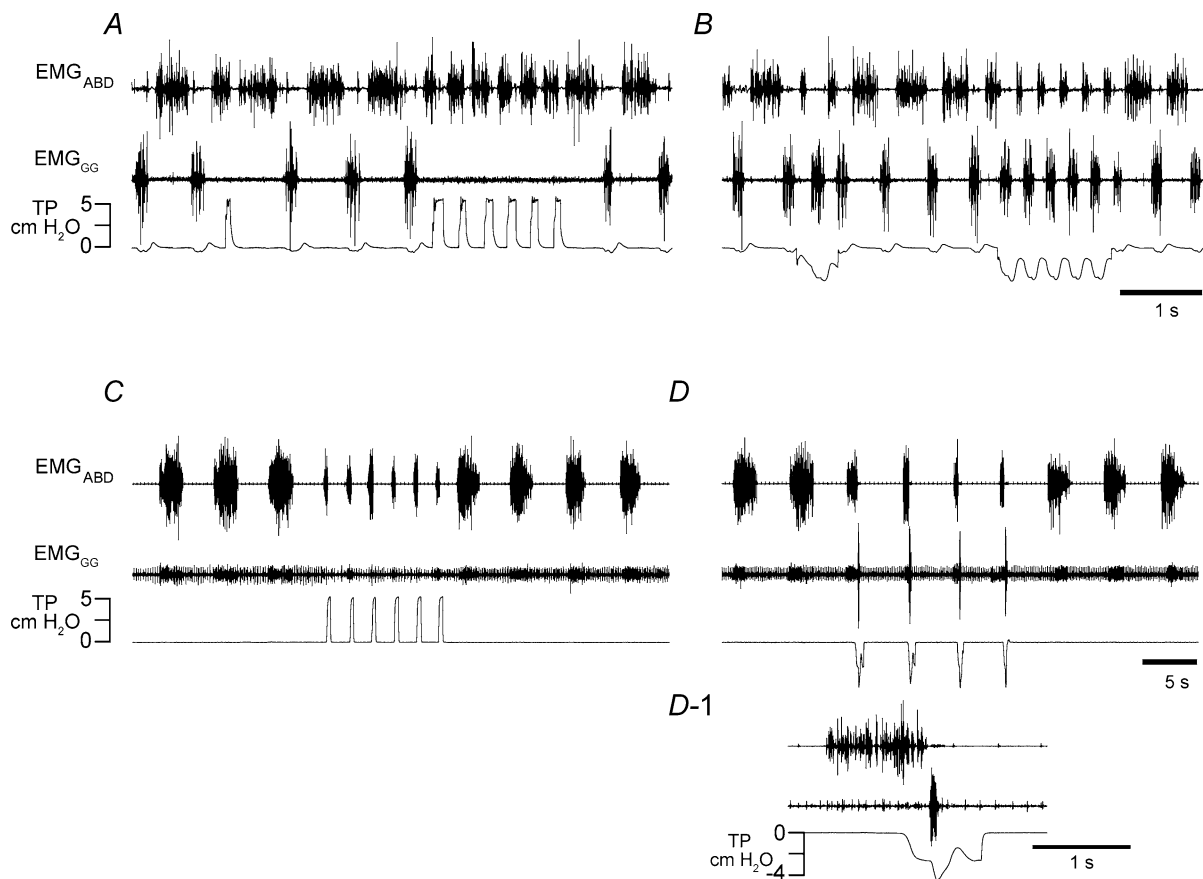


**Figure 4. Rhythmic lung inflations increased  $f_E$  and rhythmic lung deflations increased  $f_I$  in a 9-day-old rat with intact vagi given fentanyl in which all cycles were E-only**

Traces,  $\text{EMG}_{\text{ABD}}$ ,  $\text{EMG}_{\text{GG}}$  and tracheal pressure (TP). A and B, Breuer-Hering inflation/deflation reflexes before administration of fentanyl. A, inflation reflex triggered by brief lung inflations (upward deflections of TP trace) leads to apnoea and briefly inhibits  $\text{EMG}_{\text{ABD}}$  activity. B, brief lung deflation triggers an extra inspiration, and sustained lung deflation increases  $f_I$  from 92 to 208  $\text{min}^{-1}$ . C and D, after administration of fentanyl in a dose that eliminated inspiratory activity, i.e. all cycles were E-only. C, brief lung inflations applied shortly after the beginning of each  $\text{EMG}_{\text{ABD}}$  burst increased  $f_E$  from 11 to 29 bursts  $\text{min}^{-1}$  and shortened  $\text{EMG}_{\text{ABD}}$  bursts from 2.2 to 0.4 s. D, brief lung deflations triggered inspirations (indicated by further downward deflections of TP trace) and terminated ongoing  $\text{EMG}_{\text{ABD}}$  bursts, e.g. D-1. Note that  $f_E$  remained fairly constant despite shortening of  $\text{EMG}_{\text{ABD}}$  bursts. D-1, the first deflation in D on an expanded time scale. Note that  $\text{EMG}_{\text{ABD}}$  burst was not terminated until the onset of inspiration.

activity alternate, with  $f_I/f_E = 1$ . Opiates can produce a quantal pattern of breathing that significantly reduces this ratio in neonatal (Janczewski *et al.* 2002), juvenile (Mellen *et al.* 2003) and adult (Vasilakos *et al.* 2005) rats. Lung inflation further reduced this ratio, whereas lung deflation or a low dose of naloxone increased it. Brainstem transections rostral to the VII nucleus did not affect quantal breathing, whereas transections at the caudal end of the VII nucleus eliminated active expirations.

**Modified two-rhythm generator hypothesis.** In our modified two-rhythm generator hypothesis, an expiratory rhythm generator (E-rhythm generator) drives expiratory motor bursts and can remain operational when the inspiratory rhythm generator (I-rhythm generator) is depressed ( $f_I < f_E$ ), even inactivated ( $f_I = 0$ ). The two-rhythm generator hypothesis contrasts with the longstanding single-rhythm generator hypotheses that stipulate that synaptic inhibition from inspiratory (and postinspiratory) neurones underlies the rhythm of expiratory neurones; these hypotheses require that every expiratory burst be preceded by an inspiration (and postinspiration) (Richter, 1982; Sears *et al.* 1982; Bianchi *et al.* 1995); consequently these hypotheses cannot explain expiratory bursts that are not preceded by an inspiration (and post-inspiration). Consistent with the single-rhythm generator hypotheses, quantal breathing can occur if rhythmogenic inspiratory activity continues to be generated but fails to activate inspiratory motoneurones, i.e. the central inspiratory rhythm persists but fails to produce inspiratory motor output. However, our data show otherwise. (i) The loss of inspiratory motor activity

is widespread and synchronous, as the inspiratory activity of both pumping muscles, i.e. those generating inspiratory flow, and of upper airway muscles, i.e. those modulating upper airway resistance, as reflected in I-EMG<sub>GG</sub>, ceased simultaneously. The failure of a focal and radiating source of inspiratory rhythm generation (presumably the preBötC; Feldman *et al.* 2003) is a more parsimonious explanation for this observation than transmission failure that would require an anatomically widespread inhibition of inspiratory pre- and/or motoneurones. (ii) E-only cycles were shorter, with briefer EMG<sub>ABD</sub> bursts, than I-E cycles (Fig. 2). Transmission failure due to blockade of inspiratory pre- or motoneurones should not affect cycle or burst duration, at least in vagotomized rats. (iii) During I-E cycles (in vagotomized rats), EMG<sub>ABD</sub> activity was inhibited during inspiration, splitting the EMG<sub>ABD</sub> burst into two components; during E-only cycles, EMG<sub>ABD</sub> bursts were not split (Fig. 2D). (iv) In the presence of fentanyl, there could be a significant phase lag between the termination of an E-EMG<sub>GG</sub> burst and the onset of an I-EMG<sub>GG</sub> burst (Fig. 3). These effects could not be due to fentanyl-induced inhibition of inspiratory pre- or motoneurones *per se*.

We conclude that fentanyl-induced quantal breathing is due to the selective depression of the I-rhythm generator that results in the loss of activity in inspiratory premotor (Feldman, 1986; Howard & Sears, 1991; Takeda *et al.* 2001; Haji *et al.* 2003) and motor neurones. If the I-rhythm generator fails during quantal breathing, then the continuing expiratory rhythm, seen here as EMG<sub>ABD</sub> bursts and active expiratory airflow, must originate from a different rhythm generator.

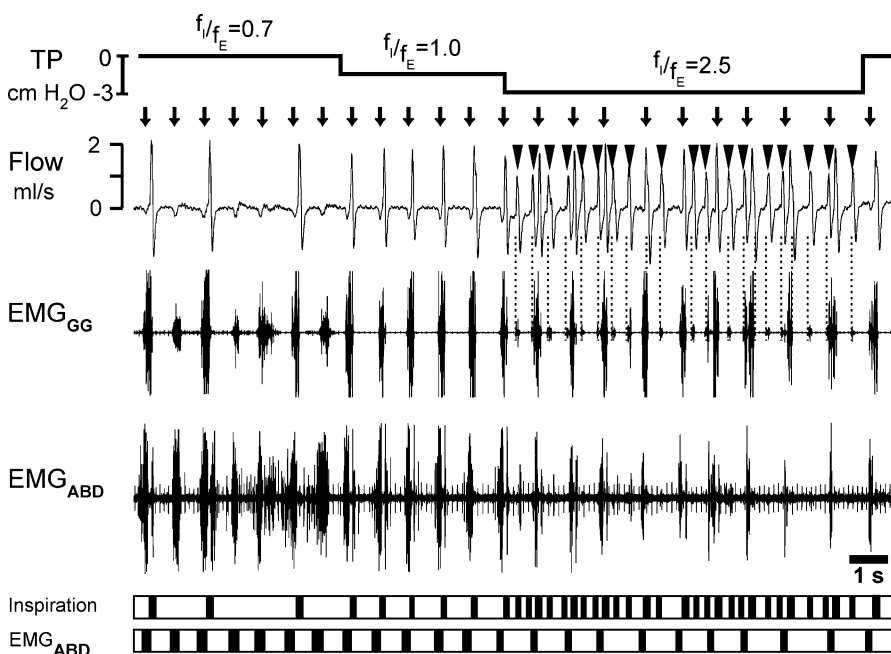


**Figure 5. Response to lung deflation in an 11-day-old rat with intact vagi and transected pons given fentanyl**

Traces, tracheal pressure (TP), respiratory flow, EMG<sub>ABD</sub>, EMG<sub>GG</sub>. Bottom, timing bars (see Fig. 1). Arrows mark onset of EMG<sub>ABD</sub> bursts. Negative pressure of  $-1.5$  cmH<sub>2</sub>O did not change  $f_E$  but did increase  $f_I$ , increasing  $f_I/f_E$  from 0.7 to 1.0. Negative pressure of  $-3$  cmH<sub>2</sub>O recruited additional inspirations (triangles/dotted lines).  $f_I$  increased leading to  $f_I/f_E = 2.5$ . The frequency of I activity locked to EMG<sub>ABD</sub> bursts was similar to that of preceding I-E cycles, and was clearly different from the rhythm of inspirations 'in between' EMG<sub>ABD</sub> bursts (triangles). Note that during lung deflation, EMG<sub>ABD</sub> bursts became shorter.

### Location of the I- and E-rhythm generators

We attempted to localize the E-rhythm generator by brainstem transections. In midbrain-transected juvenile rats, subsequent complete transection at the level of the rostral end of the VII nucleus increased  $f_E$  but did not affect the overall pattern of breathing. Thus, following these midbrain and midpontine transections: (i) an alternating pattern of inspiratory and expiratory activity remained; (ii) fentanyl could still induce quantal breathing; and (iii) the Breuer-Hering reflexes remained robust. These results indicate that expiratory rhythm is suppressed by pontine structures rostral to the VII nucleus (with the noradrenergic A5 group a likely source of inhibition; Errchidi *et al.* 1991; Viemari *et al.* 2004) and that the respiratory rhythm generator(s) lie more caudal. Subsequent transection through the caudal end of the VII nucleus eliminated  $EMG_{ABD}$  bursts, but rhythmic inspirations continued. These transections would have cut the ventral respiratory column (Alheid *et al.* 2002) at the level of the RTN/pFRG (Feldman *et al.* 2003; Onimaru & Homma, 2003).

We consider unlikely the possibility that damage to structures just caudal to the cut that eliminated expiratory activity (Fig. 7C), in particular to the BötC, could explain our results. (i) We did not observe any pathology in the BötC during histological examination (Fig. 7C, inset), although we cannot rule out subtle damage. (ii) BötC neurones are (predominately) glycinergic interneurons (Schreihofer *et al.* 1999; Ezure *et al.* 2003) and exert widespread (often monosynaptic) inhibition on respiratory pre- and motoneurone (Bianchi *et al.* 1995). We are unaware of any data that show that these neurones provide excitatory inputs to expiratory motoneurons or are rhythmogenic.

We conclude that vital components of the E-rhythm generator are within or rostral to RTN/pFRG and that the I-rhythm generator is located more caudally, presumably in the preBötC (Smith *et al.* 1991; Feldman *et al.* 2003). That there may be two rhythm generators is consistent with comparative data suggesting an emergence of a second rhythm generator with a major evolutionary transition in breathing, either from water to air breathing in vertebrate (Mellen *et al.* 2003; Vasilakos *et al.* 2005) or with the origin

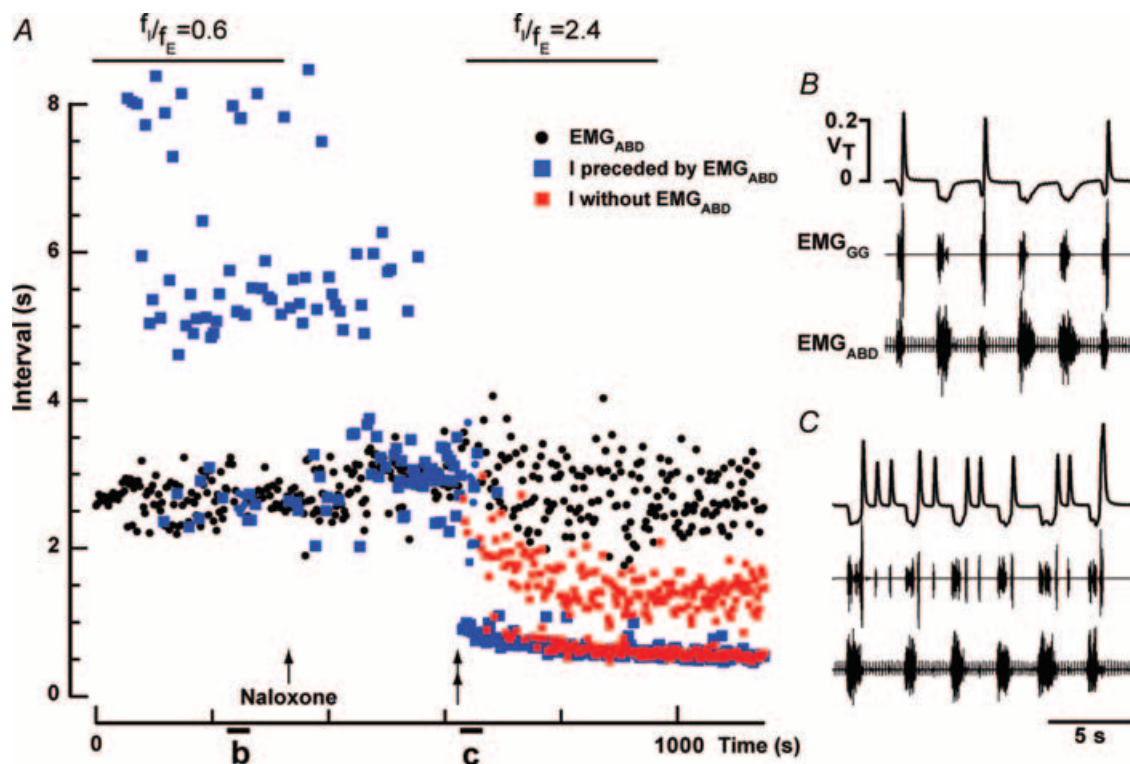


**Figure 6.** Naloxone increased  $f_1/f_E$  in an 11-day-old rat with intact vagi given fentanyl

A, intervals between successive  $EMG_{ABD}$  bursts (black circles), and between inspirations preceded (blue squares) or not preceded (red squares) by an  $EMG_{ABD}$  burst. A small dose of naloxone ( $0.03 \text{ mg kg}^{-1} \text{ s.c.}$ ) was injected (arrow) and antagonized fentanyl-induced changes in breathing apparent after  $\sim 300 \text{ s}$  (double arrow). Note that naloxone had little effect on  $f_E$ , but increased  $f_1$  to the point where some inspirations (red squares) occurred in between E-bursts. B, quantal breathing after fentanyl but before naloxone. C,  $\sim 300 \text{ s}$  after injection of naloxone, ectopic inspiratory bursts were induced.

of the diaphragm in mammals (Feldman *et al.* 2003; Mellen *et al.* 2003; Vasilakos *et al.* 2005).

**Mice with neuroanatomical defects affecting RTN/pFRG exhibit breathing problems.** Neuroanatomical defects in mice resulting from the *Hoxa1*<sup>-/-</sup> or *Krox-20*<sup>-/-</sup> mutations result in deletion or pathology of the region containing RTN/pFRG (Jacquin *et al.* 1996; del Toro *et al.* 2001; Borday *et al.* 2004). These mutant mice die within 24 h after birth due to prolonged apnoeas. Naloxone administered during the first 48 h after birth eliminates these apnoeas, ensuring long-term survival of *Krox-20*<sup>-/-</sup> mutants and some *Hoxa1*<sup>-/-</sup> mutants (Jacquin *et al.* 1996; del Toro *et al.* 2001). The respiratory disturbances in

*Krox-20*<sup>-/-</sup> mice were proposed to be due to a pathology or deletion of an 'anti-apnoea' (Jacquin *et al.* 1996) centre, most likely the RTN/pFRG (Borday *et al.* 2004), which promotes breathing immediately after birth. We suggest that in these *Hoxa1*<sup>-/-</sup> and *Krox-20*<sup>-/-</sup> mice, endogenous opiates released at birth (Grunstein *et al.* 1981; Hazinski *et al.* 1981; Chernick & Craig, 1982; Jansen & Chernick, 1983) depress the opiate-sensitive preBötC (Gray *et al.* 1999) leading to death by asphyxia in the absence of an alternative source of respiratory rhythm or the relief of this antagonism by naloxone. Thus, in normal mice, an opiate-insensitive rhythm generator in RTN/pFRG could play a critical role in assuring an adequate breathing pattern immediately after birth when there is a surge of

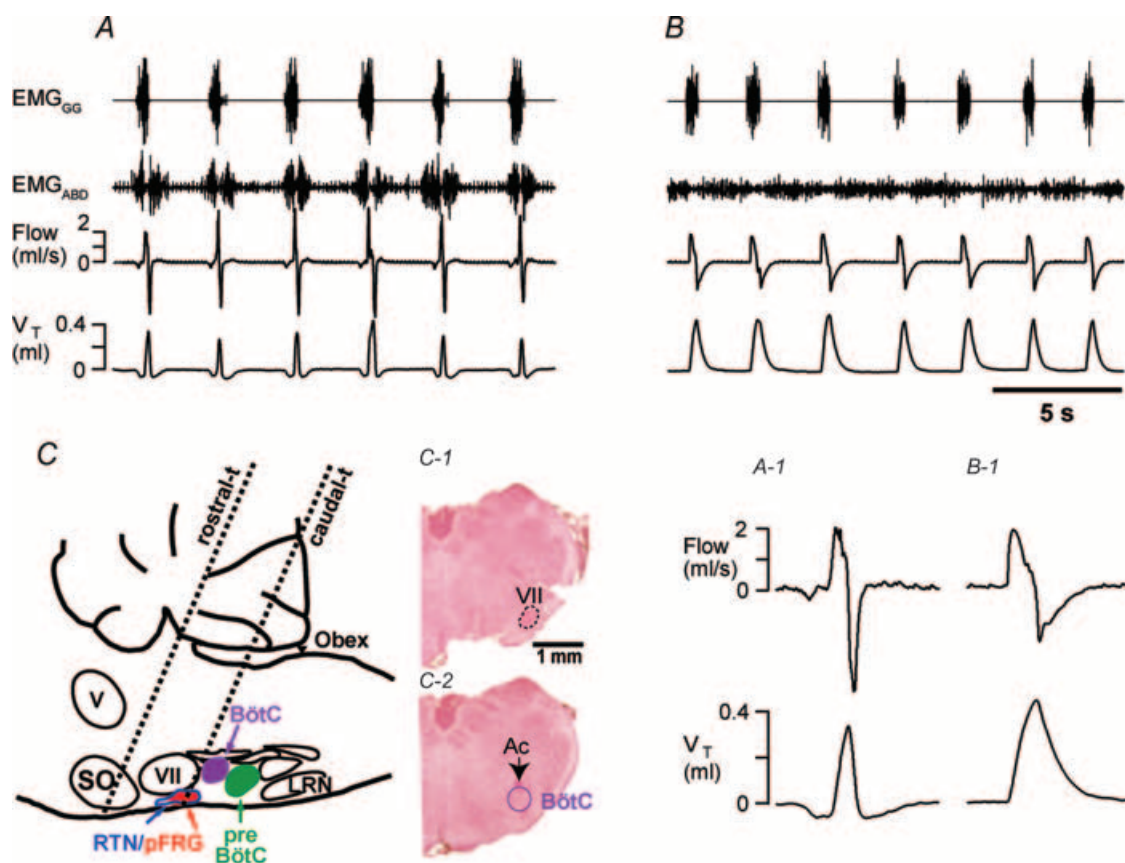


**Figure 7. Transection rostral to the facial nucleus did not affect breathing pattern, whereas transection at the caudal end of the facial nucleus eliminated EMG<sub>ABD</sub> bursts (but not inspirations) in vagotomized rats**

*A*, breathing after transection at the level just rostral to the VII nucleus (dotted line, 'rostral-t' in *C*) in rats that spontaneously recovered from quantal pattern of breathing. *B*, breathing after transection marked as 'caudal-t' in *C*. Only this most caudal transection completely eliminated EMG<sub>ABD</sub> bursts. Tonic EMG<sub>ABD</sub> activity, inhibited during inspirations, could still be observed. *A-1* and *B-2*, expanded time-scale of flow and V<sub>T</sub> during the first cycles of traces in *A* and *B*. *C*, sagittal representation of medulla and pons showing the levels of the most rostral ('rostral-t') and caudal ('caudal-t') transections. Intermediate transections were also made (see text). *C-1* and *C-2*, medullary sections (40 μm thick) of remaining medulla cut at the same angle as 'caudal-t' transection. The first section (*C-1*), showing the caudal end of the VII nucleus, was modestly damaged, but the next section (*C-2*), showing rostral end of BötC, was intact in every rat (*n* = 5). V, motor trigeminal nucleus; VII, facial nucleus; LRN, lateral reticular nucleus; preBötC, preBötzinger Complex; BötC, Bötzing Complex; pFRG, parafacial respiratory group; RTN, retrotrapezoid nucleus; SO, superior olivary complex; Ac, ambiguus nucleus compact.

endogenous opiates (Grunstein *et al.* 1981; Hazinski *et al.* 1981; Chernick & Craig, 1982; Jansen & Chernick, 1983) that wanes shortly thereafter (Hazinski *et al.* 1981).

Alternatively or in addition, the depressed breathing in these newborn mutant mice could be due to the loss of a critical *tonic* drive. In the RTN, there are chemosensitive, glutamatergic neurones (Mulkey *et al.* 2004) that would respond to an apnoea-induced increase in  $P_{\text{CO}_2}$  (Guyenet *et al.* 2005). In normal mice, their activation would increase tonic respiratory drive to preBötC neurones, acting to prevent apnoea. Absence or significant reduction of this  $\text{CO}_2$ -dependent drive in *Krox-20<sup>-/-</sup>* and *Hoxa1<sup>-/-</sup>* mice as a result of their RTN dysfunction could significantly contribute to their breathing problems at birth that would be relieved by the disinhibitory effects of naloxone on opiate-depressed preBötC neurones.

Depression of preBötC function can also be induced by targeted deletion of preBötC neurokinin 1 receptor expressing neurones (Gray *et al.* 2001). In adult rats, partial ablation of preBötC neurones induces central apnoeas during sleep (McKay *et al.* 2005) that are common in humans, especially in the elderly. The possibility that the RTN/pFRG acts to prevent/reduce these central apnoeas during sleep in adults, especially when preBötC function is partially compromised, follows from its proposed role in early postnatal life as a critical source of respiratory drive.

### Neurones driving the E-rhythm generator

On the basis of the location, firing pattern, and resistance to opioids of pre-I neurones (Onimaru *et al.* 1988, 1997; Ballanyi *et al.* 1999; Takeda *et al.* 2001; Mellen *et al.* 2003), we propose that these neurones are the E-rhythm generator kernel. Pre-I (as well as inspiratory and expiratory) neurones are routinely recorded in the RTN/pFRG *in vitro* in 0–4 days old rodents (Onimaru & Homma, 2003). Recordings of pre-I neurones in adult mammals have been problematical (Connelly *et al.* 1990; Schwarzacher *et al.* 1995; Guyenet *et al.* 2005). The majority of them are located within 150  $\mu\text{m}$  of the ventral medullary surface of the medulla in neonatal (Onimaru & Homma, 2003) and adult (Ellenberger & Feldman, 1990) rat; therefore, it may be easier to find them when approaching from the ventral surface of the medulla (Connelly *et al.* 1990; Onimaru & Homma, 2003) than when using a dorsal approach (Guyenet *et al.* 2005). In adult chloralose–urethane anaesthetized cats with robust expiratory activity, inspiratory, expiratory and respiratory-modulated double bursting neurones are found in the RTN (Connelly *et al.* 1990). The later neurones have one burst spanning the end of inspiration through the beginning of postinspiration and a second burst during active expiration (Connelly *et al.* 1990); see also (Schwarzacher *et al.* 1995). The firing pattern

of these neurones is similar but not identical to that of pre-I neurones in neonates *in vitro*; thus it is not certain whether they are the same neurones at a different stage of development (Ballanyi *et al.* 1999). In contrast, pre-I, inspiratory and expiratory neurones are not found in the RTN of halothane-anaesthetized adult rats breathing a hyperoxic gas mixture (Guyenet *et al.* 2005); however, we have not observed active expirations in rats under such experimental conditions (unpublished observation). We suggest that this observation is not simply a correlation and that rhythmicity in the RTN/pFRG is causal to the robustness of the expiratory motor activity. We postulate that bursts of expiratory motor activity originate from rhythmically active neurones in the RTN/pFRG, whereas when expiratory motor activity is weak or tonic, it is because these neurones are no longer rhythmic, and, in this case, the predominately inspiratory rhythm is driven by the preBötC.

Opioid-resistant pre-I neurones project to opioid-resistant bulbospinal premotoneurones in the caudal ventral respiratory column that drive abdominal muscle motoneurone (Janczewski *et al.* 2002). This pathway can account for the opioid-resistant bursts of  $\text{EMG}_{\text{ABD}}$  activity we observed. Moreover, in response to opioids, inspiratory motor output is eliminated after preBötC inspiratory neurones are depressed below their firing threshold; yet, these neurones still receive subthreshold excitatory/inhibitory synaptic drives, presumably from pre-I neurones (Mellen *et al.* 2003). These data support the hypothesis that fentanyl-induced quantal breathing is due to depression of the I-rhythm generator in the preBötC, which continues to receive excitatory and inhibitory inputs from the E-rhythm generator that can still trigger inspiratory bursts of activity. In *en bloc* preparations, rhythmic bursting of pre-I neurones appears to be initiated in the RTN/pFRG (Onimaru & Homma, 2003). This location and their hypothesized role in generating expiratory rhythm are in accord with our finding that transection through the VII nucleus eliminated expiratory activity.

Our hypothesis that pre-I neurones are the key constituents of the E-rhythm generator differs from the originally proposed role of these neurones as necessary and sufficient for the generation of the respiratory rhythm (Onimaru *et al.* 1988; Onimaru & Homma, 2003).

During quantal slowing of breathing in the juvenile rats, every inspiration is preceded by an  $\text{EMG}_{\text{ABD}}$  burst, but some  $\text{EMG}_{\text{ABD}}$  bursts are not followed by inspiratory activity (Figs 1–6). We suggest that the E-rhythm generator paces the respiratory network when the excitability of the I-rhythm generator is low and that of the E-rhythm generator is high, such as in *in vitro en bloc* preparations or in intact rodents exposed to opiates. Other conditions that suppress the I- but not the E-rhythm generator should result in  $f_{\text{I}} < f_{\text{E}}$ . Indeed, partial ablation of preBötC

neurons in awake adult goats can result in inspiratory apnoea with rhythmic abdominal activity (Wenninger *et al.* 2004). Moreover, in awake infants and young children, sudden noxious stimuli can cause inspiratory apnoea with persistence of rhythm in abdominal muscles (Southall *et al.* 1985).

However, we suggest that the E-rhythm generator does not pace respiratory rhythm when the excitability of the I-rhythm generator is normal or elevated, or the E-rhythm generator is depressed, as might be the case in anaesthetized mammals at CO<sub>2</sub> levels just above threshold to produce inspiratory activity (Guyenet *et al.* 2005) but not active expiration. Values of  $f_I/f_E > 1$  in response to extra excitation of inspiratory activity, elicited by lung deflation or a low dose of naloxone, indicate that the I-rhythm generator is capable of generating faster rhythms than the E-rhythm generator. This effect of naloxone is likely to be mediated by preBötC neurons that express  $\mu$ -opiate receptors (Gray *et al.* 1999; Mancke *et al.* 2003).

When several inspirations followed an EMG<sub>ABD</sub> burst, the one immediately succeeding the burst had a larger amplitude (Fig. 5), which is consistent with an excitatory role of pre-I neurons on one subpopulation of inspiratory neurons (Onimaru *et al.* 1997) and also with the hypothesis that they are not essential to drive inspiratory activity.

### Coordination of two-rhythm generators

The coordination of respiratory pattern will rely on, in addition to whatever direct interactions there are between the two hypothesized rhythm generators, shared inputs, such as from peripheral afferents, neuromodulatory systems, e.g. substance P, serotonin and norepinephrine, and common descending inputs related to emotion, volition, etc. An example in this study of a key peripheral afferent coordinating the respiratory pattern is vagal afferents underlying the Breuer-Hering reflexes.

In summary, we hypothesize that the respiratory network is composed of two separate rhythm generators, with one or the other capable of dominating the behaviour by generating a faster rhythm depending on their relative levels of excitability, which may vary with state, chemoreceptor drive, afferent input, and development in intact mammals, and with details of experimental preparation in laboratory studies.

### References

Alheid GF, Gray PA, Jiang MC, Feldman JL & McCrimmon DR (2002). Parvalbumin in respiratory neurons of the ventrolateral medulla of the adult rat. *J Neurocytol* **31**, 693–717.

Ballanyi K (2004). Neuromodulation of the perinatal respiratory network. *Curr Neuropharmacol* **2**, 221–243.

Ballanyi K, Onimaru H & Homma I (1999). Respiratory network function in the isolated brainstem–spinal cord of newborn rats. *Prog Neurobiol* **59**, 583–634.

Bianchi AL, Denavit-Saubie M & Champagnat J (1995). Central control of breathing in mammals: neuronal circuitry, membrane properties, and neurotransmitters. *Physiol Rev* **75**, 1–45.

Borday C, Wrobel L, Fortin G, Champagnat J, Thaeron-Antono C & Thoby-Brisson M (2004). Developmental gene control of brainstem function: views from the embryo. *Prog Biophys Mol Biol* **84**, 89–106.

Brainerd EL (1999). New perspectives on the evolution of lung ventilation mechanisms in vertebrates. *Experimental Biology Online* **4**, 11–28.

Chernick V & Craig RJ (1982). Naloxone reverses neonatal depression caused by fetal asphyxia. *Science* **216**, 1252–1253.

Connelly CA, Ellenberger HH & Feldman JL (1990). Respiratory activity in retrotrapezoid nucleus in cat. *Am J Physiol* **258**, L33–L44.

del Toro ED, Borday V, Davenne M, Neun R, Rijli FM & Champagnat J (2001). Generation of a novel functional neuronal circuit in Hoxa1 mutant mice. *J Neurosci* **21**, 5637–5642.

Drummond GB (2003). The abdominal muscles in anaesthesia and after surgery. *Br J Anaesth* **91**, 73–80.

Ellenberger HH & Feldman JL (1990). Brainstem connections of the rostral ventral respiratory group of the rat. *Brain Res* **513**, 35–42.

Errchidi S, Monteau R & Hilaire G (1991). Noradrenergic modulation of the medullary respiratory rhythm generator in the newborn rat: an *in vitro* study. *J Physiol* **443**, 477–498.

Ezure K, Tanaka I & Kondo H (2003). Glycine is used as a transmitter by decrementing expiratory neurons of the ventrolateral medulla in the rat. *J Neurosci* **23**, 8941–8948.

Feldman JL (1986). Neurophysiology of breathing in mammals. In *Handbook of Physiology, The Nervous System Intrinsic Regulatory Systems of the Brain*, ed. Mountcastle VB, Bloom FE, Geiger SR, pp. 463–524. American Physiological Society, Bethesda, Maryland.

Feldman JL & Cowan JD (1975). Large-scale activity in neural nets II: a model for the brainstem respiratory oscillator. *Biol Cybern* **17**, 39–51.

Feldman JL, Mitchell GS & Nattie EE (2003). Breathing: rhythmicity, plasticity, chemosensitivity. *Annu Rev Neurosci* **26**, 239–266.

Gray PA, Janczewski WA, Mellen N, McCrimmon DR & Feldman JL (2001). Normal breathing requires preBötzinger Complex neurokinin-1 receptor-expressing neurons. *Nat Neurosci* **4**, 927–930.

Gray PA, Rekling JC, Bocchiaro CM & Feldman JL (1999). Modulation of respiratory frequency by peptidergic input to rhythmogenic neurons in the preBötzinger Complex. *Science* **286**, 1566–1568.

Grillner S (1991). Recombination of motor pattern generators. *Current Biol* **1**, 231–233.

Grillner S & Wallen P (2002). Cellular bases of a vertebrate locomotor system – steering, intersegmental and segmental co-ordination and sensory control. *Brain Res Rev* **40**, 92–106.

- Grunstein MM, Hazinski TA & Schlueter MA (1981). Respiratory control during hypoxia in newborn rabbits: implied action of endorphins. *J Appl Physiol* **51**, 122–130.
- Guyenet PG, Mulkey DK, Stornetta RL & Bayliss DA (2005). Regulation of ventral surface chemoreceptors by the central respiratory pattern generator. *J Neurosci* **25**, 8938–8947.
- Haji A, Okazaki M, Ohi Y, Yamazaki H & Takeda R (2003). Biphasic effects of morphine on bulbar respiratory neuronal activities in decerebrate cats. *Neuropharmacology* **45**, 368–379.
- Hazinski TA, Grunstein MM, Schlueter MA & Tooley WH (1981). Effect of naloxone on ventilation in newborn rabbits. *J Appl Physiol* **50**, 713–717.
- Homi HM, Mixco JM, Sheng H, Grocott HP, Pearlstein RD & Warner DS (2003). Severe hypotension is not essential for isoflurane neuroprotection against forebrain ischemia in mice. *Anesthesiology* **99**, 1145–1151.
- Howard RS & Sears TA (1991). The effects of opiates on the respiratory activity of thoracic motoneurons in the anaesthetized and decerebrate rabbit. *J Physiol* **437**, 181–199.
- Jacquin TD, Borday V, Schneider-Maunoury S, Topilko P, Ghilini G, Kato F, Charnay P & Champagnat J (1996). Reorganization of pontine rhythmogenic neuronal networks in Krox-20 knockout mice. *Neuron* **17**, 747–758.
- Janczewski WA & Feldman JL (2002).  $\mu$ -Opioid receptor agonist suppresses rhythmic inspiratory (I) but neither pre-inspiratory nor expiratory activity in the newborn rat. Program no. 221.11. Society for Neuroscience, Washington, DC.
- Janczewski WA & Feldman JL (2003). Two distinct generators drive the respiratory network; both generators are inhibited by lung inflation and excited by hypoxia. Program no. 2412. Society for Neuroscience, Washington, DC.
- Janczewski WA & Karczewski WA (1984). Respiratory effects of pontine, medullary and spinal cord midline sections in the rabbit. *Respir Physiol* **57**, 293–305.
- Janczewski WA & Karczewski WA (1990). The role of neural connections crossed at the cervical level in determining rhythm and amplitude of respiration in cats and rabbits. *Respir Physiol* **79**, 163–175.
- Janczewski WA, Onimaru H, Homma I & Feldman JL (2002). Opioid-resistant respiratory pathway from the preinspiratory neurones to abdominal muscles: *in vivo* and *in vitro* study in the newborn rat. *J Physiol* **545**, 1017–1026.
- Jansen AH & Chernick V (1983). Development of respiratory control. *Physiol Rev* **63**, 437–483.
- Katz RI, Lagasse RS, Levy A & Alexander G (1993). Hemodynamic stability and patient satisfaction after anesthetic induction with thiopental sodium, ketamine, thiopental-fentanyl, and ketamine-fentanyl. *J Clin Anesth* **5**, 134–140.
- Kudo N & Yamada T (1987). *N*-methyl-D, L-aspartate-induced locomotor activity in a spinal cord-hindlimb muscles preparation of the newborn rat studied *in vitro*. *Neurosci Lett* **75**, 43–48.
- Madsen J, Cold G, Hansen E, Bardrum B & Kruse-Larsen C (1987). Cerebral blood flow and metabolism during isoflurane-induced hypotension in patients subjected to surgery for cerebral aneurysms. *Br J Anaesth* **59**, 1204–1207.
- Manzke T, Guenther U, Ponimaskin EG, Haller M, Dutschmann M, Schwarzacher S & Richter DW (2003). 5-HT<sub>4</sub>(a) receptors avert opioid-induced breathing depression without loss of analgesia. *Science* **301**, 226–229.
- McKay LC, Janczewski WA & Feldman JL (2005). Sleep-disordered breathing after targeted ablation of preBotzinger complex neurons. *Nat Neurosci* **8**, 1142–1144.
- Mellen N, Janczewski WA, Bocchiaro CM & Feldman JL (2003). Opioid-induced quantal slowing reveals dual networks for respiratory rhythm generation. *Neuron* **37**, 821–826.
- Mulkey DK, Stornetta RL, Weston MC, Simmons JR, Parker A, Bayliss DA & Guyenet PG (2004). Respiratory control by ventral surface chemoreceptor neurons in rats. *Nat Neurosci* **7**, 1360–1369.
- Onimaru H, Arata A & Homma I (1988). Primary respiratory rhythm generator in the medulla of brainstem–spinal cord preparation from newborn rat. *Brain Res* **445**, 314–324.
- Onimaru H, Arata A & Homma I (1997). Neuronal mechanisms of respiratory rhythm generation: an approach using *in vitro* preparation. *Jpn J Physiol* **47**, 385–403.
- Onimaru H & Homma I (2003). A novel functional neuron group for respiratory rhythm generation in the ventral medulla. *J Neurosci* **23**, 1478–1486.
- Porter R (1970). *Breathing: Hering Breuer Centenary Symposium, Ciba Foundation Symposium*. Churchill, London.
- Richter DW (1982). Generation and maintenance of the respiratory rhythm. *J Exp Biol* **100**, 93–107.
- Richter DW, Ballanyi K & Schwarzacher S (1992). Mechanisms of respiratory rhythm generation. *Curr Opin Neurobiol* **2**, 788–793.
- Ringaert K & Mutch W (1988). Regional cerebral blood flow and response to carbon dioxide during controlled hypotension with isoflurane anesthesia in the rat. *Anesth Analg* **67**, 383–388.
- Rybak IA, Paton JF & Schwaber JS (1997). Modeling neural mechanisms for genesis of respiratory rhythm and pattern. II. Network models of the central respiratory pattern generator. *J Neurophysiol* **77**, 2007–2026.
- Sakamoto T, Kawaguchi M, Inoue S & Furuya H (2001). Suppressive effect of nitrous oxide on motor evoked potentials can be reversed by train stimulation in rabbits under ketamine/fentanyl anaesthesia, but not with additional propofol. *Br J Anaesth* **86**, 395–402.
- Schreihofer AM, Stornetta RL & Guyenet PG (1999). Evidence for glycinergic respiratory neurons: Bötzing neurons express mRNA for glycinergic transporter 2. *J Comp Neurol* **407**, 583–597.
- Schwarzacher SW, Smith JC & Richter DW (1995). Pre-Bötzinger complex in the cat. *J Neurophysiol* **73**, 1452–1461.
- Sears TA, Berger AJ & Phillipson EA (1982). Reciprocal tonic activation of inspiratory and expiratory motoneurons by chemical drives. *Nature* **299**, 728–730.
- Smith JC, Ellenberger HH, Ballanyi K, Richter DW & Feldman JL (1991). Pre-Bötzinger complex: a brainstem region that may generate respiratory rhythm in mammals. *Science* **254**, 726–729.

- Southall DP, Talbert DG, Johnson P, Morley CJ, Salmons S, Miller J & Helms PJ (1985). Prolonged expiratory apnoea: a disorder resulting in episodes of severe arterial hypoxaemia in infants and young children. *Lancet* **2**, 571–577.
- Takeda S, Eriksson LI, Yamamoto Y, Joensen H, Onimaru H & Lindahl SG (2001). Opioid action on respiratory neuron activity of the isolated respiratory network in newborn rats. *Anesthesiology* **95**, 740–749.
- Tanabe A, Fujii T & Onimaru H (2005). Facilitation of respiratory rhythm by a  $\mu$ -opioid agonist in newborn rat pons–medulla–spinal-cord preparations. *Neurosci Lett* **375**, 19–22.
- Vasilakos K, Wilson RJ, Kimura N & Remmers JE (2005). Ancient gill and lung oscillators may generate the respiratory rhythm of frogs and rats. *J Neurobiol* **62**, 369–385.
- Viemari JC, Bevington M, Coulon P & Hilaire G (2004). Nasal trigeminal inputs release the A5 inhibition received by the respiratory rhythm generator of the mouse neonate. *J Neurophysiol* **91**, 746–758.
- Wenninger JM, Pan LG, Klum L, Leekley T, Bastastic J, Hodges MR, Feroah TR, Davis S & Forster HV (2004). Large lesions in the pre-Botzinger complex area eliminate eupneic respiratory rhythm in awake goats. *J Appl Physiol* **97**, 1629–1636.
- Wixson SK & Smiler KL (1997). *Anesthesia and Analgesia in Rodents: American College of Laboratory Animal Medicine 1990 Forum*. Academic Press, San Diego, London.

## Acknowledgements

This work was supported by National Institutes of Health Grant HL 70029.

## Supplemental material

The online version of this paper can be accessed at:

DOI: 10.1113/jphysiol.2005.098848

<http://jp.physoc.org/cgi/content/full/jphysiol.2005.098848/DC1> and contains the following supplemental material:

Supplemental Fig. 1. Quantal pattern of breathing and reflex responses to positive (CPAP) and negative airway pressure in juvenile rat with intact vagi and given fentanyl

Supplemental Video 1. Response to Breuer-Hering inflation reflex (CPAP, +4 and +9 cmH<sub>2</sub>O) during quantal pattern of breathing in an 8-day-old rat with intact vagi and given fentanyl

Supplemental Video 2. Response to Breuer-Hering deflation reflex (pressures, –1 and –4 cmH<sub>2</sub>O) during quantal pattern of breathing in an 8-day-old rat with intact vagi and given fentanyl

This material can also be found as part of the full-text HTML version available from <http://www.blackwell-synergy.com>

**Distinct rhythm generators for inspiration and expiration in the juvenile rat**  
Wiktor A. Janczewski and Jack L. Feldman

*J. Physiol.* 2006;570;407-420; originally published online Nov 17, 2005;

DOI: 10.1113/jphysiol.2005.098848

**This information is current as of January 19, 2006**

<b>Updated Information &amp; Services</b>	including high-resolution figures, can be found at: <a href="http://jp.physoc.org/cgi/content/full/570/2/407">http://jp.physoc.org/cgi/content/full/570/2/407</a>
<b>Related Articles</b>	A related article has been published: <a href="http://jp.physoc.org/cgi/content/full/570/2/207">http://jp.physoc.org/cgi/content/full/570/2/207</a>
<b>Supplementary Material</b>	Supplementary material can be found at: <a href="http://jp.physoc.org/cgi/content/full/jphysiol.2005.098848/DC1">http://jp.physoc.org/cgi/content/full/jphysiol.2005.098848/DC1</a>
<b>Permissions &amp; Licensing</b>	Information about reproducing this article in parts (figures, tables) or in its entirety can be found online at: <a href="http://jp.physoc.org/misc/Permissions.shtml">http://jp.physoc.org/misc/Permissions.shtml</a>
<b>Reprints</b>	Information about ordering reprints can be found online: <a href="http://jp.physoc.org/misc/reprints.shtml">http://jp.physoc.org/misc/reprints.shtml</a>